Vibration Analysis for the Comfort Assessment of Superyachts

Tatiana Pais[1*], Lorenzo Moro[2], Dario Boote[1] and Marco Biot[3]

1. Diten Department, University of Genoa, Genoa, 16145, Italy
2. Department of Ocean and Naval Architectural Engineering, Memorial University of Newfoundland, St John, NL A1B 3X9, Canada
3. Department of Engineering and Architecture, University of Trieste, Trieste, 34127, Italy

Abstract: Comfort levels on modern superyachts have recently been the object of specific attention of the most important Classification Societies, which issued new rules and regulations for evaluating noise and vibration maximum levels. These rules are named "Comfort Class Rules" and set the general criteria for noise and vibration measurements in different vessels' areas, as well as the maximum noise and vibration limit values. As far as the vibration assessment is concerned, the Comfort Class Rules follow either the ISO 6954:1984 standard or the ISO 6954:2000. After an introduction to these relevant standards, the authors herein present a procedure developed to predict the vibration levels on ships. This procedure builds on finite element linear dynamic analysis and is applied to predict the vibration levels on a 60 m superyacht considered as a case study. The results of the numerical simulations are then benchmarked against experimental data acquired during the sea trial of the vessel. This analysis also allows the authors to evaluate the global damping ratio to be used by designers in the vibration analysis of superyachts.

Keywords: added mass, structural damping, dynamic finite element analysis, sea trial, superyacht, dynamic analysis of ship structures, comfort analysis

1 Introduction

Yacht designers and builders are continuously looking for new solutions to reduce construction costs and improve the quality of their vessels (Boote *et al.,* 2013). With regard to superyachts of over 30 m in length, performances are no more a primary objective, and the efforts of shipbuilders are mostly focused on other aspects, such as aesthetic impact and on-board comfort. From this point of view, vibration and noise represent challenging issues that ship designers have to deal with since the initial phase of the project. Indeed, an early analysis of the ship structural dynamics can prevent the shipyard from increasing construction costs and in avoiding onerous structural modifications when the ship structures are already built.

Given the objective difficulty in making any change to the dynamic behavior of the hull structure after construction, performing accurate Finite Element (FE) predictive analyses to identify the natural frequencies of the hull and local structures (*i.e.*, decks and bulkheads) and their dynamic response to exciting loads induced by propellers, engines, and waves is extremely important (Moro *et al*., 2013; Asmussen, 2001).

Several studies were performed in the recent years to develop an effective procedure for the simulation of the structural dynamics of ships and the vibration levels on the main ship's areas. These studies focused on the characterization of the main sources and the dynamic response of the ship structures. Propellers generate excitation forces that are transmitted into the ship via the shaft line and in the form of pressure fluctuations acting on the ship hull (Cho *et al.,* 2015). Several methods for the prediction and simulations of propeller-induced hull vibration were developed and studied. Holden *et al*. (1980) developed an empirical method based on the analysis of full-scale measurements undertaken on 72 ships. Ligtelijn *et al.* (2004) more recently benchmarked the outcomes of computational simulations and model tests against the outcomes of full-scale tests performed on five different types of ships. Lee *et al.* (2013) studied the correlation between the cavitation-induced pressure fluctuation measurements in a cavitation tunnel and full-scale measurements. Lee *et al.* (2014) combined hydrodynamic and hydro-acoustic methods to estimate the hull pressure fluctuation induced by propeller sheet cavitation. Even though these studies provided insight into the numerical and experimental methods for the prediction of propeller-induced hull pressure fluctuation, an effective method to predict this phenomenon is still missing. Other researchers focused their activities on the development of methods for the characterization of reciprocating machinery installed on ships. Biot *et al.* (2015) proposed a method for the characterization of the reciprocating machinery foundation. This method can be used to study the vibration generated by marine diesel engines in the audio frequency range using the single-point-approach (Biot *et al.,* 2014). Meanwhile, Moro *et al.* (2015) proposed a method to simulate the dynamic response of resilient mounting systems. This method can be used to predict the vibration generated by marine diesel engines that are resiliently mounted.

This study presents the first results of an ongoing research activity developed in a joint collaboration among the Naval Architecture Section of the DITEN Department of the University of Genova, the Department of Ocean and Naval

Accepted date: 10 Mar-2017

***Corresponding author Email:** tatianapais@hotmail.it

Architectural Engineering of Memorial University of Newfoundland, and the Department of Engineering and Architecture of the University of Trieste. The research activity aims to provide insights in the most relevant aspects related to hull structural dynamics and effective countermeasures to control vibration on ships.

After a discussion on the most relevant international standards and rules on ship vibration and comfort assessment, the authors herein present a procedure that builds on the numerical FE simulations of ship structures to predict the vibration levels on ships. The procedure presented in this work is also used to predict the damping ratio ξ to be used in the vibration analysis of superyachts for the comfort assessment.

2 ISO Standards for the evaluation of vibration on ships

The International Organization for Standardization (ISO) has issued standards that set the procedure for the assessment of the vibration level on merchant vessels as well as the maximum vibration limits. The evaluation methodologies of ship vibration ranges within the low frequency range (1-200 Hz) and the set of vibration limits are provided in the two versions of the Standard ISO 6954 (ISO 1984; ISO 2000). The first issue of this regulation dates back in 1984, from which the term ISO 6954:1984 was introduced. The latest review occurred on 2000. Hence, the code was named ISO 6954:2000.

The 1984 version did not have a large support (adopted with 9 votes out of 17). The introduction of the 2000 revision approved in the context of the Working Group 2, sub-committee 2, Technical Committee 108 of the ISO (acronym ISO TC180/SC2/WG2) has given rise to an ongoing debate between the supporters of its validity and its detractors.

Hereinafter, the two versions of the ISO 6954 are discussed and compared to identify their main advantages and disadvantages

2.1 ISO 6954:1984

The ISO 6954:1984 was issued to provide ship designers with guidelines for the vibration measurements on board merchant vessels over 100 m (ISO 6954:1984). The standard sets the procedure for the hull vibration measurement starting from ISO 4867 and ISO 4868, while the assessment of the human impact is based on the ISO 2631-1. Fig. 1 shows the admissible range of vibrations from situations commonly accepted on board and measured over time. The limit values have a bi-linear trend decreasing between 1 and 5 Hz and is constant between 5 and 100 Hz.

As shown in Table 1, the limit values are expressed in acceleration and velocity peaks. The standard defines the maximum repetitive value (MRV) to achieve the peak values from the measured r.m.s. values. The MRV is calculated as follows:

$$\mathrm{MRV} = C_F \cdot \sqrt{2} \cdot V_{\mathrm{rms}} \tag{1}$$

where ($C_F \cdot \sqrt{2}$) is the crest factor, and CF is the conversion factor. According to the standard, the conversion factor ranges between 1.0 for pure stationary sinusoidal vibration and 1.8.

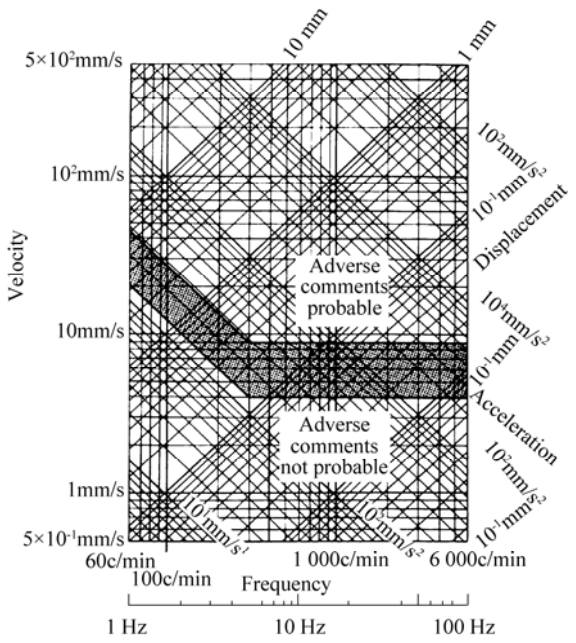

Fig. 1 Vibration limits according to ISO 6954:1984

Table 1 Vibration limits according to ISO 6954:1984

ISO 6954:1984	Frequency range	
	1-5 Hz	5-100 Hz
Values above which adverse comments are probable	Peak acceleration 285 mm/s^2	Peak velocity 9 mm/s
Values above which adverse comments are not probable	Peak acceleration 126 mm/s^2	Peak velocity 4 mm/s

The value to be assigned to the CF coefficient is still the subject of a long and lively debate. A relevant criticism to the ISO 6954:1984, which was formulated in the report of the ISSC 2006 Committee II.2—Dynamic Response (ISSC 2016) in relation to the definition of the MRV, cannot be easily defined, could be a source of ambiguity in the vibration assessment and development of a procedure to clearly identify the MRV, and is still under investigation (Brocco *et al.,* 2015). The situation does not improve in case the MRV is deducted from the r.m.s. value ($V_{\mathrm{r.m.s.}}$). Indeed, the standard does not specify the bandwidth and the average time record to be measured for the MRV evaluation and does not define a robust procedure to evaluate CF. Moreover, the MRV can be obtained from a frequency spectrum if the latter is known. In this case, its value varies depending on the acquisition parameters (e.g., block size and resolution), thereby increasing the uncertainty on the outcomes of the measurement surveys.

The concept of overall frequency-weighted r.m.s. was introduced in 1997 to address the multi-frequency phenomena with a crest factor CF lower than 9. The typical vibration signals measured on-board are generally well below this value. The definition of a generic quantity g in terms of the overall frequency-weighted r.m.s in time domain or in spectral terms is defined as follows (ISO 2631-1, 1997):

$$g_w = \sqrt{\frac{1}{T}\cdot\int_0^T g_w^2(t)\mathrm{d}t} \tag{2}$$

$$g_w = \sqrt{\sum_i (W_i g_i)^2} \tag{3}$$

where T is the period of the time record; g_w is the weighted quantity (acceleration or velocity); W_i is the weight function of the ith band; and g_i is the r.m.s value of the ith frequency band.

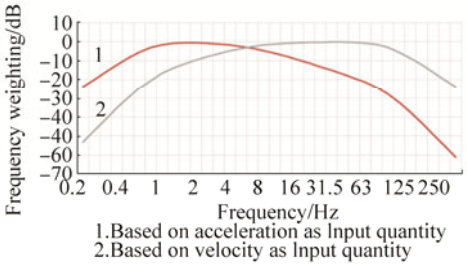

Fig. 2 Combined frequency-weighting curves

Fig. 2 shows the plots of the weighting function W_i when acceleration and velocity are considered as input quantities. This approach has rapidly spread in the study of human exposure to vibration (ISO 2631-1, 1997) and the habitability of areas on vessels (ISO 2631-2, 1989). The measurements performed according to this procedure provide results that are highly insensitive compared to those obtained by measurements performed according to the version of the standard issued in 1984, which means that the ambiguity and the arbitrariness related to the definition of the MRV have been removed. Moreover, the introduction of high-quality and powerful digital acquisition systems allows the overall analysis of the acquired data and the integration on the entire frequency range, which does not affect the diagnostic capabilities provided by the acquisition in narrowband specified by the previous ISO. All the reasons listed above led to the alignment of rule ISO 6954 to this new approach in 2000.

2.2 ISO 6954:2000

The ISO 6954:2000 regulates the measurement and evaluation of vibrations from 1 to 80 Hz on merchant and passenger ships regardless of their length. The procedure presented in this standard focuses on the comfort assessment of the different areas on ships that are divided into three different categories as follows:

A: passenger cabins;

B: crew areas; and

C: workspaces.

The analysis of the data acquired to ISO 6954:2000 must be performed according to ISO 8041 and ISO 2631-1. Table 2 shows the admissible range of vibration in terms of the overall frequency-weighted r.m.s. According to this standard, the measurements should be taken in the three translational directions at least in two measurement points on each deck of the ship.

Table 2 Vibration limits according to ISO 6954:2000

ISO 6954:2000	Area classification					
	A		*B*		*C*	
	Acceleration/ ($mm\cdot s^{-2}$)	Velocity/ ($mm\cdot s^{-1}$)	Acceleration/ ($mm\cdot s^{-2}$)	Velocity/ ($mm\cdot s^{-1}$)	Acceleration/ ($mm\cdot s^{-2}$)	Velocity/ ($mm\cdot s^{-1}$)
Values above which adverse comments are probable	143	4	214	6	286	8
Values above which adverse comments are not probable	71.5	2	107	3	143	4

2.3 Design aspects

ISO standard 6954:1984 presents a suitable formulation that allows the designers to include the vibratory aspect in the design procedure. The advantage of the 1984 approach is that the dynamic response of the vessel can be assessed with respect to the maximum exciting force by fixing a limit for a single harmonic component among the possible exciting forces. This means that the calculations are reduced to determine the dynamic response of the ship excited by the first propeller blade frequencies, first axial exciting frequencies of the propeller, and engine- and cylinder-firing rates of the prime engines. These input data for the simulation of the ship structural dynamics are usually available in the early design stage, and can be performed using an FE analysis.

A standard that does not provide the designers with the ability to predict and control the quality of the product with a reasonable accuracy in the early design stages clearly constitutes an issue. In some cases, this is what happens with ISO 6954:2000 final outcomes. Indeed, the energy approach integrates the whole frequency band of the measured vibration levels, implying that all the harmonic contributions within the frequency range 1–80 Hz are included in the analysis. This approach is not easily

manageable in numerical analyses because the characteristics of the sources, the capability to reproduce the vibratory response of the vessel, and the analysis of outcomes of the simulations in terms of the weighted velocity levels are not directly identifiable. Generally speaking, the exciting frequencies that can be found in the frequency ranges 1 and 80 Hz are as follows:

- multiple harmonics of the fundamental blade pass propeller;
- broadband contribution resulting from cavitation effects; and
- higher harmonics of the fundamental frequencies of the main machinery.

According to the newest ISO Standard, all these contributions should be estimated in advance in terms of intensity and frequency, then added and weighted. The values obtained in this analysis should later be compared with the proposed thresholds.

One of the challenges of this approach is the high uncertainty on the simulation of cavitating propellers in a dynamic structural analysis.

Without focusing on the complex cavitation problems, different types of cavitation can be observed in the marine propellers. The first one consists of phenomena located on the blade surface: bubble, sheet, and cloud cavitation. The second one is related to flow turbulence phenomena: tip or hub vortex cavitation and hull vortex cavitation. The sheet cavitation is generally responsible for the presence of a high harmonic frequency of the blade, which is usually up to the fifth harmonic component, while tip vortex cavitation and breaking vortex cavitation would be the source of broadband noise on a limited frequency range. Nowadays, the intensity of the first two harmonics of the blade frequency is predictable with good reliability. Meanwhile, the estimation of the higher harmonics is still affected by a significant uncertainty. The determination of the broadband noise generated by the tip vortex cavitation is affected by the lack of knowledge on the generating mechanisms and the elements that contribute to produce it, as for example, the viscosity, compressibility, and inhomogeneity of the wake.

For design purposes, the procedures proposed by the standards should be compatible with the technical resources of the yards. Moreover, the standard requires that the entire energy content of the main sources and of the dynamic structural response should be considered. This significantly increases the level of uncertainty in the prediction. Indeed, the identification of the vibration sources that generate high vibration levels of the ship structures and of the effective solutions to mitigate these excessive vibration levels becomes more complex using this approach.

3 Finite element model

The case study analyzed in this paper is a 54 m-long and 9.5 m-wide superyacht built by the Italian shipyard Benetti in Livorno (Italy), and kindly made available for the present study. The FE modeling of the ship structures is the most laborious and time consuming part of a dynamic analysis. All the parts of the vessel should be modeled with equal care and attention as a function of the results to be achieved. Since the objective of this study was to perform global and local analyses, each structural component is accurately reproduced: main structures, as bulkheads and decks, primary reinforces, as beams and girders, secondary reinforcements. As far as hierarchically-lower-elements are concerned, such as brackets and fire bars, they are generally neglected. To take into consideration their weight an increase of thickness of the coherent panel is introduced. The hull geometry and structure lay out is imported from a 3D model previously created by a rendering software, as shown in Fig. 3.

Fig. 3 3D model of the superyacht considered as a case study

In Fig. 4, the numerical model of the yacht as realized in MSC.Patran Software is shown. Two types of element are used: Beam and Shell elements (MSC.Nastran 2013). The mesh was created using shell elements for plating and main reinforcements such as keelsons, floors and girders. The secondary stiffeners have been modelled using beam elements.

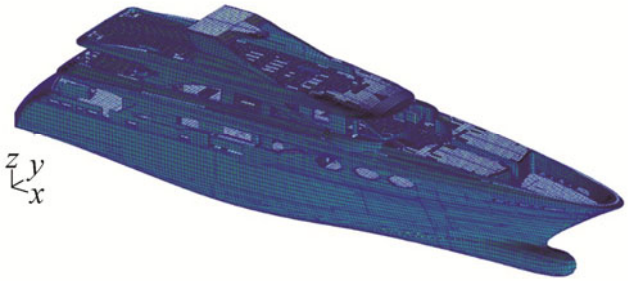

Fig. 4 FE 3D model of the superyacht considered as case study in the analysis

The numerical model of the yacht consists of 119 907 elements, 72 916 nodes and 396 144 DOFs.

Non-structural masses can be defined as distributed or lumped masses. All masses smaller than 1 kg/m^2, including insulating materials, flooring, marble, pipes, cables, filler, painting, and furniture, were applied as distributed loads (Fig. 5). Higher weights were applied to the numerical

model as lumped masses on points, where the weight insists on. Fig. 6 presents the gearbox and electric generator masses.

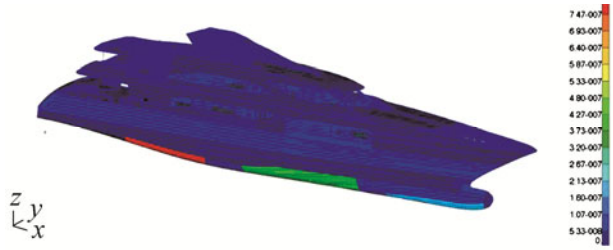

Fig. 5 Distributed masses applied to the FE model of the superyacht

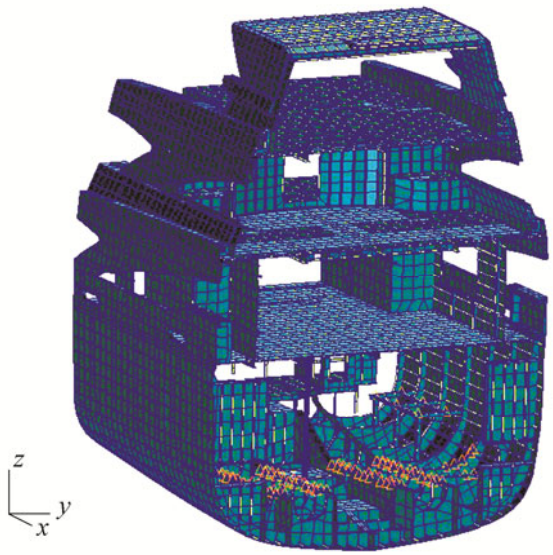

Fig. 6 Examples of the lumped masses applied to the FE model of the superyacht

A frequency response analysis should be performed to evaluate the vibration levels of a superyacht structure excited by steady-state oscillatory excitations. The harmonic loads representing the oscillatory excitation forces induced by the vibration sources were applied to the FE model of the ship's structures to perform this analysis. The natural frequencies and the mode shapes were computed by solving an eigenvalue problem. The response of the ship structures can be obtained by solving the following equation of motion as follows:

$$\boldsymbol{M}\{\ddot{\boldsymbol{u}}(t)\}+\boldsymbol{C}\{\dot{\boldsymbol{u}}(t)\}+\boldsymbol{K}\{\boldsymbol{u}(t)\}=\{\boldsymbol{F}(t)\} \quad (4)$$

where $\boldsymbol{M}$ is the mass matrix; $\{\ddot{\boldsymbol{u}}(t)\}$ is the acceleration vector; $\boldsymbol{C}$ is the damping matrix; $\{\dot{\boldsymbol{u}}(t)\}$ is the velocity vector; $\boldsymbol{K}$ is the stiffness matrix; $\{\boldsymbol{u}(t)\}$ is the displacement vector; and $\{\boldsymbol{F}\}$ is the harmonic forces vector. We can calculate the vibration levels on each point of the ship's structure by solving Eq. (4).

3.1 Estimation of the added mass

Ships are subjected to considerable inertial effects because of the high density of the fluid in which they operate. When moving, the ship drags with her a significant portion of water. The mass of which can be considered associated to the ship mass. This water mass is then called "added mass" (Korotkin, 2007). The hydrodynamic added mass is usually of considerable entity. As an example, in the case of a sphere immersed in a fluid moving perpendicularly to the free surface, the added mass is equal to half the mass displaced by the sphere itself. As a consequence, the presence of the added mass cannot be neglected in a ship vibration analysis. In the 30s of the last century, Burrill (1935) elaborated an initial empirical formulation of the first vertical mode of vibration of a ship as follows:

$$N_v=\varphi\cdot\sqrt{\frac{I}{(\Delta+\Delta_1)\cdot L^3\cdot(1+N_s)}} \quad (5)$$

where N_v is the frequency of the first mode of vertical vibration expressed in cycles per minute; I is the momentum of inertia of the main section expressed in feet; Δ is the displacement expressed in tons; Δ_1 is the added mass; L is the ship length between the perpendiculars; N_s is the shear correction factor of Lockwood Taylor; and φ is an empiric constant. As it is possible to note in the above equation, the added mass plays a decisive role in determining the natural frequencies of a ship. Different methodologies for determining the term Δ_1 are available, but the Lewis method still remains the most used (Lewis, 1929).

3.1.1 Added mass calculation according to the Lewis method

The added mass associated to the numerical model for the vertical plane motions is manually calculated using the Lewis formulation (Korotkin, 2007). This methodology involves the identification of hydrodynamic masses, which are calculated per unit of length and integrated over the length of the immersed body providing the total added mass. Lewis provides a series of curves, which return a Lewis coefficient depending on the shape of a generic section and from the quantity $\frac{B(x)/2}{T(x)}$ to identify the sectional added masses.

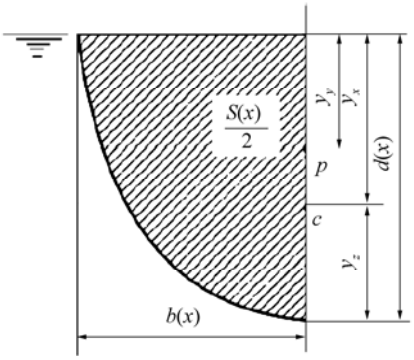

Fig. 7 Scheme of (half of) the immersed part of a shipframe (Korotkin, 2007)

After the total added mass is calculated, it is multiplied by a corrective coefficient J introduced to take into account the 3D effects acting on the body. The formulas for calculating the mass addition are illustrated hereinafter (Korotkin 2007).

Given a ship section, the following dimensions are

defined in Fig. 7 as:

d(x) is the draught;

$b(x)$ is the half breadth of the ship section at waterline;

$S(x)$ is the area of the immersed part of the shipframe;

p is the centroid of the immersed part of the ship section area; and

c is the position of the center of torsion at ship hull vibrations.

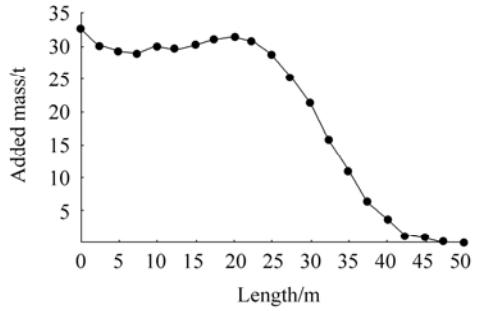

Fig. 8 Added mass calculated for each shipframe of the superyacht

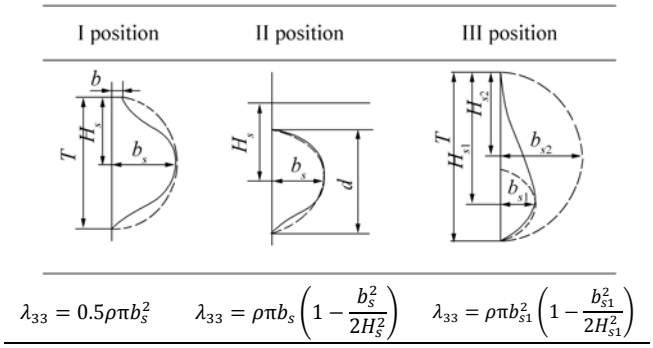

Fig. 9 Added mass for the bulb-type ship sections (Korotkin 2007)

The following entities are introduced:

$$\sigma(x)=\frac{S(x)}{2b(x)d(x)} \qquad q=\frac{d(x)}{b(x)} \tag{6}$$

and the following auxiliary coefficients are defined:

$$a=\frac{1}{2}\left[3(1+q)-\sqrt{1+10q+q^2-\frac{32\sigma q}{\pi}}\right] \tag{7}$$

$$c_v=1+(1+q-a)\cdot(q-a) \tag{8}$$

where c_v is the sectional two-dimensional (2D) added mass coefficient, also known as the Lewis-form coefficient.

The added masses of the ship sections in the vertical direction can be found using the following formula:

$$\lambda_{33}=J_n c_v\left(\frac{\pi}{2}\rho b^2\right) \tag{9}$$

The index n in Eq. (9) indicates that the added mass is dependent on the vibration mode. In this case, the reduction J factor is defined as follows:

$$J_n=1.02-3\left(1.2-\frac{1}{n}\right)\frac{B}{L} \tag{10}$$

where B is the water line breadth amidships, and L is the ship length. The formula is only applied to vertical modes with n = 2–5. The length of the yacht was dived into 20 equidistant sections. The graph of Fig. 8 shows the section 2D added mass coefficient, c_v, obtained from Eq. (8). Fig. 9 shows the added mass for the bulb-type ship sections.

The total sectional 2D added mass equal to 1005 tons is multiplied by the correction factor defined in Eq. (10). Table 3 shows the added mass for each mode shape.

Table 3 Overall added mass value for each mode shape

Mode shape	J_n	λ_{33}/t
1	0.67	673.68
2	0.59	589.89
3	0.55	547.99
4	0.52	522.86

3.1.2 Numerical computation of the added mass

The numerical methods for the calculation of the added mass are available nowadays and implemented in commercial FE packages. The boundary element method is considered in the case of the MSC.Nastran software (MSC.Nastran, 2013).

MSC.Nastran is provided with a special function that allows the consideration of the possible presence of fluids inside and/or outside the model. The command is called MFLUID and considers the boundary element method. A brief overview of the well-known theory of the Boundary Element Method (BEM) for the computation of the added mass is given.

The relationship between the fluid pressure field and the interface acceleration can be defined via potential flow theory, in which the velocity potential function $\varnothing(\boldsymbol{x})$ satisfies the Laplace equation $\nabla^2\varnothing=0$ to obtain the fluid forces on the structure. The boundary condition is $\varnothing\to 0$ at free surface and infinite and $\nabla\varnothing\cdot\boldsymbol{n}=\frac{\mathrm{d}\boldsymbol{\delta}}{\mathrm{d}t\cdot\boldsymbol{n}}$ on the solid surface, where $\boldsymbol{\delta}$ is the surface displacement, and $\boldsymbol{n}$ is the surface normal.

The field potential is written in the following form (Faltisen, 1990):

$$\varnothing(\boldsymbol{x})=\int_{\Gamma}G(\boldsymbol{x},\boldsymbol{y})\sigma(\boldsymbol{y})\mathrm{d}\Gamma(\boldsymbol{y})=\sum_{j=1}^{N}\sigma_j\int_{\Gamma}G(\boldsymbol{x},\boldsymbol{y}_j)\mathrm{d}\Gamma(\boldsymbol{y}_j) \tag{11}$$

where $\boldsymbol{y}$ is the coordinate vector of a point on a panel, as shown in Fig. 10; σ is the source strength; and $G(\boldsymbol{x},\boldsymbol{y})=\frac{1}{|\boldsymbol{x}-\boldsymbol{y}|}$ is the fundamental solution of the Laplacian for a source of strength of 4π.

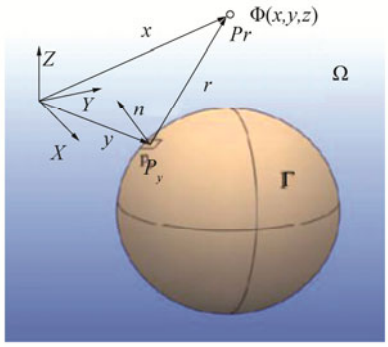

Fig. 10 Immersed solid body (Bašić *et al.* 2013)

The gradient of the velocity potential $\nabla\emptyset$ must satisfy the boundary conditions at the control points. Hence, the evaluation of Eq. (11) leads to the two following matrices:

$$\{\emptyset\}=[\boldsymbol{L}]\{\sigma\} \tag{12}$$

$$\{v\}=[\boldsymbol{\chi}][\boldsymbol{\sigma}] \tag{13}$$

where $[\boldsymbol{L}]$ and $[\boldsymbol{\chi}]$ are the coefficient matrices, which relate source strength to the control point potential and the control point fluid normal velocities, respectively. The vector $\boldsymbol{v}$ represents fluid velocities normal to the panels that can be represented using the transformation matrix $[\boldsymbol{D}]$ that contains factored direction cosines between the panel normal and global axes containing factored direction cosines between the panel normal and global axes $\{\boldsymbol{v}\} = [\boldsymbol{D}]\{\dot{\boldsymbol{u}}\}$.

The pressure field in fluid can be determined with Bernoulli theory. The pressure is integrated over the structure interface by a simple product with the diagonal matrix of panel areas $[\boldsymbol{A}]$ to provide the control point forces as follows:

$$\{F\} = \rho[A]\{\dot{\emptyset}\} \tag{14}$$

The added fluid mass matrix $[\boldsymbol{M}^f]$ may now be defined as follows:

$$\{F\} = [\boldsymbol{M}^f]\{\ddot{u}\} \tag{15}$$

The added mass is added to Eq. (4) as follows to obtain the global equation of motion of the system:

$$[\boldsymbol{M} + \boldsymbol{M}^f]\{\ddot{\boldsymbol{u}}(t)\} + [\boldsymbol{C}]\{\dot{\boldsymbol{u}}(t)\} + [\boldsymbol{K}]\{\boldsymbol{u}(t)\} = \{\boldsymbol{F}(t)\} \tag{16}$$

3.1.3 Comparison between the analytical and numerical methods

The modal analysis was performed with and without considering the added mass. Fig. 11 shows the first mode at 7.32 Hz of the dry structure. Fig. 12 presents the corresponding wet first mode at the 4.89 Hz frequency.

The only way to verify the added mass in the FE calculations in MSC.Nastran is to compare the dry and wet natural frequencies. The displacement of the superyacht is 552 t. The added mass is obtained using the following equation (Burrill, 1935):

$$\lambda_{33,n} = \Delta\left[\left(\frac{\omega_{n,\text{dry}}}{\omega_{n,\text{wet}}}\right)^2 - 1\right] \tag{17}$$

In Table 4, the first theoretical value of Table 3 are compared with the FEM value obtained by Equation 17 and Error % is calculated.

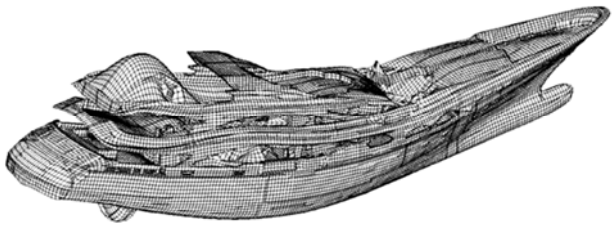

Fig. 11 First mode of the dry structure of the superyacht, 7.32 Hz

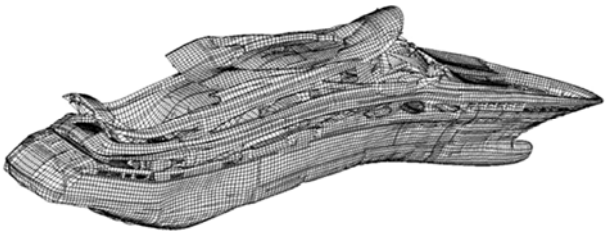

Fig. 12 First mode of the wet structure of the superyacht, 4.89 Hz

Table 4 Comparison of the added mass values calculated according to the Lewis theory and the BE method

Mode shape	ω_{dry}/ (rad·s^{-1})	ω_{wet}/ (rad·s^{-1})	λ_{33} FEM/t	λ_{33} Theoretical/t	$\Delta\lambda_{33}$/%
1	45.99	30.73	684.3	673.68	1.55

3.2 Estimation of the structural damping

The prediction of the natural frequencies of ship structures requires a precise assessment of mass and stiffness. Considerable uncertainties exist in the evaluation of the damping effects when it comes to the frequency response analysis of the ship structures excited by on-board sources (e.g., propellers and/or main engines) (ISSC 2006).

The damping may be explicit as a dashpot device that provides discrete damping at a specific location, or it can be a general inherent loss mechanism, such as the friction in joints or micro-mechanic effects within the material of a structure. The vibrational energy is dissipated as heat. These general damping phenomena are not precisely defined and, consequently, are not easily quantified leading to the definition of overall levels or smear type damping, either for the entire structure or by region, grouping materials with similar characteristics. The damping caused by these effects is generally low and warrants simple approximations. Linear–elastic materials exhibit two types of damping: viscous and structural. The viscous damping force is proportional to velocity, and the structural damping force is proportional to displacement. The structural damping was

studied in this case (De Silva, 2007).

The structural damping force is proportional to the displacement and is given as:

$$f_s = G \cdot k \cdot u \tag{18}$$

where G is the structural damping coefficient, and k is the structural stiffness.

While the material damping only depends on the energy dissipation caused by the deformation of the material used for the ship structure, the total damping referred to as structural damping depends on the dissipative effects caused by rigid and movable connections of the components and masses acting on the structure itself (Moro *et al*., 2013). The latter may be classified as component damping if it accounts for the contribution on damping given by (Pais *et al*., 2016):

- floor coverings or fittings, or cargo damping, if it covers the action of large bodies in contact with structures, like fluid or solid in bulk and container filled with different types of goods;
- hydrodynamic damping, when related to energy dissipation in liquids with a free surface.

The structural damping effect is not easy to be defined and may increase the material damping factor with amplifications up to 10 (ISSC, 2006). The structural damping value to be considered in the frequency analysis of a boat must be set according to the type of analysis, that is, the level at which the analysis is performed: hull substructure or local vibration. In fact, local damping has a very small influence on the vibration amplitudes of the hull in the lower frequency range. Therefore, while in a local analysis, the structural damping needs to be accurately set considering the local reasons of energy dissipation in a global analysis, where only relevant damping sources need to be accounted for. Different parameters can be used to characterize the damping properties of the structure. In the case study presented in this paper, damping is expressed as follows in terms of the damping ratio:

$$\xi = \frac{c}{c_c} \tag{19}$$

where c is the damping coefficient, and c_c is the critical damping defined as follows:

$$c_c = 2\sqrt{km} \tag{20}$$

where k is the stiffness, and m is the mass.

In the scientific literature, several empirical formulas are available for a rough estimation of the damping value to be used in the dynamic structural analysis of ship structures. In fact, the damping coefficient grows as the vibration frequency increases. Germanischer Lloyd provided a graph for container ships to identify a damping ratio for the FE dynamic simulation of ship structures (Asmussen *et al.* 2001). No indication is provided in the case of pleasure boats. Hereinafter, an iterative procedure for the estimation of the damping ratio to be used in the structural dynamic analysis of a superyacht is presented.

4 Full-scale vibration measurement

A full-scale measurement survey was performed to assess the on-board comfort in relation to vibration. The measured data were acquired during the sea-trial of the vessel according to the standard ISO 6954:1984. The data were acquired in the time domain using accelerometers ICP controlled by an eight-channel data acquisition system. The data were analyzed in real-time in the frequency domain. Hence, the researchers were able to check the quality of the measures and identify the eventual unwanted input vibration (e.g., unexpected impacts). Three 1 m-long records were acquired for each measurement point. The resulting spectra were then averaged to improve the quality of the outcomes. Table 5 shows the on-board positions of the measurement points. The measurement surveys were performed at the cruising speed of the vessel (V = 12 kn) according to ISO 6954:1984. The measured vibration levels were expressed in r.m.s. values for the purpose of this study, thereby allowing the researchers a direct benchmark of the simulation outcomes against the measured data. Figs. 13 to 17 show the spectra of the velocity levels measured on-board during the sea trials of the vessel. All the velocity-measured vibration velocities were lower than the limits set in ISO 6954:1984.

Table 5 Position of the measurement points on the superyacht

# Measurement Point	Position
35	Main deck
40	Main deck
101	Upper deck
104	Upper deck
201	Sun deck

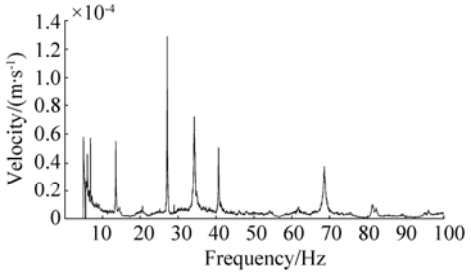

Fig. 13 Velocity spectrum measured in measurement point 35

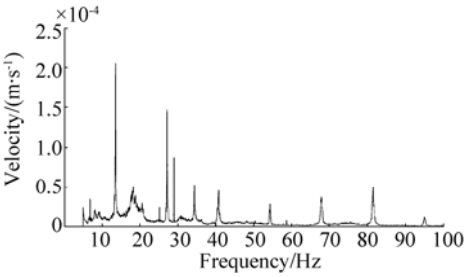

Fig. 14 Velocity spectrum measured in measurement point 40

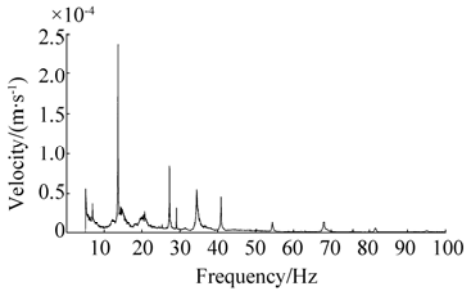

Fig. 15 Velocity spectrum measured in measurement point 101

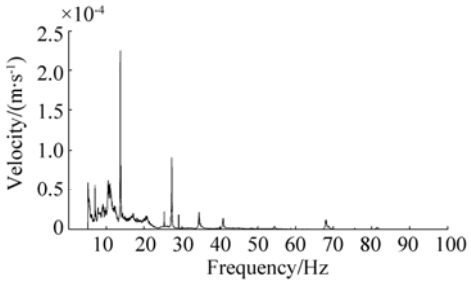

Fig. 16 Velocity spectrum measured in measurement point 104

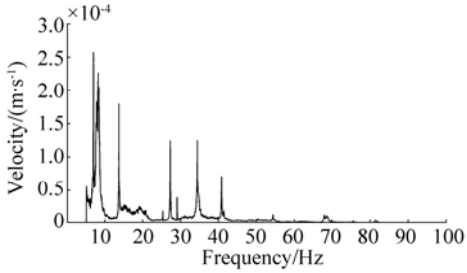

Fig. 17 Velocity spectrum measured in measurement point 201

5 Procedure for the overall damping ratio evaluation

The FE model presented in Section 2 was used by the authors to evaluate the damping ratio for use in the structural dynamic simulations to evaluate the on-board vibration levels in the different areas of the vessel. These results were obtained by performing linear dynamic FE analyses.

The vibration sources considered in these simulations were the two propellers. The maximum propeller-induced hull pressure was provided by the shipyard and measured in tow testing: 1 kPa for the half loaded propeller and 2 kPa for the propeller 100% loaded.

The propeller-induced hull pressure was assumed to be sinusoidal with a frequency equal to a blade pass frequency (BPF) of 35.25 Hz. The propeller-induced hull pressure was applied to the vessel in an area equal to the propeller disk area (Fig. 18).

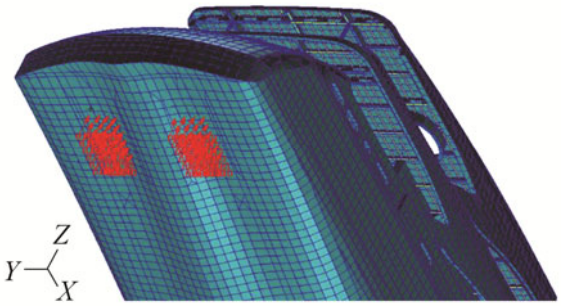

Fig. 18 Propeller-induced hull pressure fluctuation applied to the FE model of the superyacht

The proper damping ratio to be used in the simulations for the evaluation of the onboard vibration levels was obtained by performing a series of dynamic linear analyses in Nastran. The propeller-induced hull pressure fluctuation was particularly applied to the model (Fig. 18). The vibration levels at the BPF in each relevant point of the structure were calculated by performing a frequency response analysis of the vessel's structures. The damping ratio ξ in this series of simulations was increased from a starting value of 0.5% up to 10%. The outcomes of these simulations were then post-processed in MATLAB to evaluate the difference of the velocity levels calculated with the measured ones ($\Delta V_{\text{r.m.s.}}$). As an example, Fig. 19 shows the spectrum of the velocity levels acquired in measurement point 40 (Table 5). The measured signal was filtered using a high-pass filter characterized by a cutoff frequency equal to 5 Hz to neglect the effect of the ship motions. In the figure, the bold points denote the simulation outcomes. Only three points were reported for clarity. These points corresponded to the velocity levels calculated using a damping ratio ξ equal to 5%. The highest values shown in the figure were 7% and 10%. A damping ratio ξ equal to 10% minimized the difference between the calculated velocity levels and the measured ones. The quantity $\Delta V_{\text{r.m.s.}}$ calculated in measurement point 40 was plotted in Fig. 20 for the different values of damping ratios ξ.

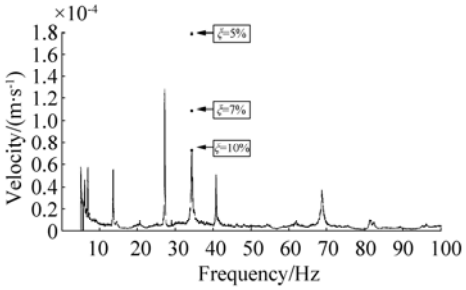

Fig. 19 Spectrum of the vibration velocity measured in measurement point 35 and outcomes of the numerical simulations at the blade pass frequency for three different values of the damping ratio ξ

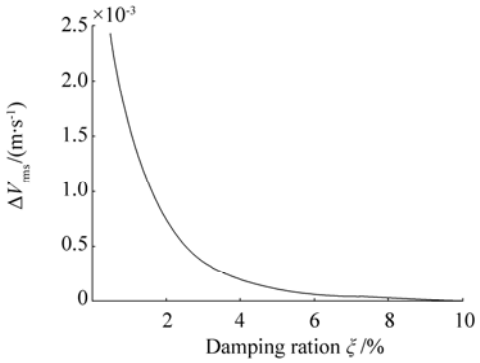

Fig. 20 Difference of the velocity levels calculated and measured $\Delta V_{\text{r.m.s.}}$ in measurement point 35 for different values of the damping ratio ξ

Table 6 Comparison of the $\Delta V_{\text{r.m.s}}$ velocity for different points

ξ /%	$\Delta V_{\text{r.m.s.}}$ velocity/(mm·s^{-1})				
	Point 35	Point 40	Point 101	Point 104	Point 201
0.5	5.59	3.46	5.69	2.41	9.59
1.0	3.80	2.22	3.90	1.62	7.28
1.5	2.82	1.56	2.92	1.07	5.79
2.0	2.26	1.15	2.36	0.72	4.65
2.5	1.90	0.86	2.00	0.50	3.77
3.0	1.66	0.66	1.76	0.36	3.08
3.5	1.48	0.51	1.58	0.26	2.53
4.0	1.34	0.39	1.44	0.19	2.10
4.5	1.23	0.30	1.33	0.14	1.76
5.0	1.13	0.23	1.23	0.11	1.49
6.0	0.97	0.12	1.07	0.06	1.08
7.0	0.84	0.06	0.94	0.04	0.81
8.0	0.74	0.01	0.84	0.03	0.61
9.0	0.64	0.00	0.74	0.02	0.47
10.0	0.56	0.00	0.66	0.01	0.37

This procedure was applied to the data obtained for each measurement point. Table 6 shows the analysis results in terms of the difference of the r.m.s. values of the velocity levels calculated and measured ($\Delta V_{\text{r.m.s.}}$) as a function of the damping ratio ξ used in the numerical simulations.

The analysis outcomes showed that $\Delta V_{\text{r.m.s}}$ was minimized for a value of the damping ratio ξ equal to 9%–10%. With the value suggested by the guidelines for the vibration analysis of the main Classification Societies, if we compare this damping ratio value, we noticed that it was generally higher. For example, the Germanischer Lloyd suggested a damping ratio equal to 8% for use in a frequency analysis higher than 20 Hz (Asmussen *et al.*, 2001). This discrepancy in the damping ratios found by the authors and suggested by the Classification Societies was explained by the fact that the latter provided values for use in the analysis of container vessels and cargo vessels. Comfort is a key factor to be competitive in the yacht market. Hence, damping and insulating materials are usually applied to the vessel vessels structures, and decks are often equipped with floating floors that isolate the living areas from the ship structures. These materials increase the overall damping of the structures, explaining the higher values of damping ratios found in this study.

6 Conclusion

This study presented the first part of a research program performed by a collaboration of the University of Genova, Memorial University of Newfoundland, and the University of Trieste. The study aimed for a deep analysis of the structural dynamics of modern superyachts to develop an accurate design procedure for the dynamic simulations of the ship structures and effective solutions to improve comfort on board in relation to noise and vibration. An overview of the recent standards issued by the ISO and the Classification Societies rules has been presented in this paper to highlight the most important parameters to be considered in the vibrational comfort assessment of superyachts. The authors later presented a procedure based on numerical FE simulations for the vibrational comfort assessment of a superyacht. The procedure was applied to a case study used to evaluate two methods for the added mass evaluation. The results of the measurement surveys acquired in the sea trials were used to validate the outcomes of the FE simulations and evaluate a damping ratio value for use to predict on-board vibration levels. The study outcomes show that a damping ratio equal to 10% should be used to properly simulate the on-board vibration levels generated by propellers.

The future development of this research activity will be the evaluation of a damping ratio considering other on-board sources and the development of a proper model for the simulation of the effect of visco-elastic materials and other devices used to increase the damping of the ship structures and isolate the on-board sources.

References

Asmussen I, Menzel W, Mumm H, 2001. *Ship vibration*. Germanischer Lloyd, Hamburg.

Bašić J, Parunov J, 2013. Analytical and numerical computation of added mass in ship vibration analysis. *Brodogradnja*, **64**(2), 1-11.

Biot M, Boote D, Brocco E, Mendoza Vassallo PN, Moro L, Pais T, 2014. Validation of a design method for the simulation of the mechanical mobility of marine diesel engine seatings. *Transport Means Proceedings of 18th International Conference*, Klaipeda, Kaunas, Lithuania.

Biot M, Boote D, Brocco E, Moro L, Pais T, Delle Piane S, 2015. Numerical and experimental analysis of the dynamic behavior of main engine foundations. *Proceedings of the Twenty-fifth (2015) International Ocean and Polar Engineering Conference (ISOPE)*, Kona, Big Island, Hawaii, USA.

Boote D, Pais T, Delle Piane S, 2013. Vibration of superyacht structures, *Proc 4th International Conference on Marine Structures*, Espoo, Finland.

Brocco E, Moro L Mendoza Vassallo PN, Biot M, Boote D, Pais T, Camporese E, 2015. Influence of the sea action on the measured vibration levels in the comfort assessment of mega yachts. *Proc. 5th International Conference on Marine Structures*, Southampton, UK.

Burrill LC, 1935. *Ship vibration: simple methods of estimating critical frequencies.* North East Coast Institution of Engineers and Shipbuilders.

Cho DS, Brizzolara S, Chirica I, Düster A, Ergin A, Hermundstad OA, Holtmann M, Hung C, Ivaldi A, Ji C, Joo WH, Leira B, Malenica S, Ogawa Y, Vaz MA, Vredeveldt A, Xiong Y, Zhan D, 2015. Committee II.2–Dynamic Response. *19th International Ship and Offshore Structures Congress ISSC*, Lisbon.

Faltinsen OM, 1990. *Sea loads on ships and offshore structures.* Cambridge Ocean Technology Series.

De Silva CW, 2007. *Vibration: fundamentals and practice.* 2nd ed. CRC Press, Taylor & Francis Group, Boca Raton, USA,.

Holden KO, Fagerjord O, Frostad R, 1980. Early design-stage approach to reducing hull surface force due to propeller cavitation. *SNAME Transactions*, **88**, 403-442.

ISO 2631-1, 1997. Mechanical vibration and shock–evaluation of human exposure to whole-body vibration–Pt 1: General requirements.

ISO 2631-2, 1989. Evaluation of human exposure to whole-body vibration - Part 2: Continuous and shock-induced vibrations in buildings (1 to 80 Hz).

ISO 4867, 1984. Code for the measurement and reporting of shipboard vibration data.

ISO 4868, 1984. Code for the measurement and reporting of local vibration data of ship structures and equipment.

ISO 6954, 1984, Mechanical vibration and shock - guidelines for the overall evaluation of vibration in merchant ships.

ISO 6954, 2000. Mechanical vibration - Guidlines for the measurement, reporting and evaluation of vibration with regard to habitability on passenger and merchant ships.

ISO 8041, 1990. Human response to vibration - Measuring instrumentation.

ISSC, 2006. *Proceedings of the 16th International Ship and Offshore Structures Congress, Report II.2 Committee, Dynamic Response*, Southampton, UK.

ISSC, 2012. *Proceedings of the 18th International Ship and Offshore Structures Congress, Report V.8 Committee, Yacht Design,* Rostock, Germany.

Korotkin AI, 2007. *Added masses of ship structures: fluid mechanics and its applications*, **88**, Springer, Berlin.

Lee JH, Han JM, Park HG, Seo JS, 2013. Improvements of model-test method for cavitation-induced pressure fluctuation in marine propeller. *Journal of Hydrodynamics*, **25**, 599-605.

Lee KH, Lee J, Kim D, Kim K, Seong W, 2014. Propeller sheet cavitation source modeling and inversion. *Journal of Sound and Vibration*, **333**, 1356-1368.

Lewis FM, 1929. The inertia of the water surrounding in a vibrating ship. *Trans. SNAME*, **37**, 1-20.

Ligtelijn JT, Van Wijngaarden HCJ, Moulijn JC, Verkuyl JB, 2004. Correlation of cavitation: comparison of full-scale data with results of model tests and computations. *SNAME 2004 Annual Meeting*. Washington, DC, USA.

Moro L, Biot M, Brocco E, De Lorenzo F, Mendoza Vassallo PN, 2013. Hull vibration analysis of river boats. *International Conference IDS2013- Amazonia*, Iquitos, Peru.

Moro L, Le Sourne H, Brocco E, Mendoza Vassallo PN, Biot M, 2015. Numerical simulation of the dynamic behavior of resilient mounts for marine diesel engines. *5th International Conference on Marine Structures MARSTRUCT*, Southampton, UK.

MSC.Nastran, 2013. Dynamic analysis User's Guide, MSC Software.

Pais T, Boote D, Kaeding P, 2016. Experimental and numerical analysis of absorber materials for steel decks. Proceedings of the Twenty-sixth (2016) *International Ocean and Polar Engineering Conference (ISOPE)*, Rodi, Greece.